

1 Reconstructing exposures from biomarkers using exposure-pharmacokinetic  
2 modeling – A case study with carbaryl

3 Kathleen Brown<sup>1§</sup>, Martin Phillips<sup>2§</sup>, Christopher Grulke<sup>3</sup>, Miyoung Yoon<sup>4</sup>, Bruce Young<sup>5</sup>, Robin  
4 McDougall<sup>6</sup>, Jeremy Leonard<sup>7</sup>, Jingtao Lu<sup>7</sup>, William Lefew<sup>8</sup>, Yu-Mei Tan<sup>1\*</sup>

5 <sup>1</sup>U.S. Environmental Protection Agency, National Exposure Research Laboratory, Durham, NC

6 <sup>2</sup> Minnesota Department of Health, St. Paul, MN

7 <sup>3</sup> Lockheed Martin, Durham, NC

8 <sup>4</sup>The Hamner Institutes for Health Sciences, Durham NC

9 <sup>5</sup>Bayer CropScience, Durham NC

10 <sup>6</sup>Astra Zeneca, Boston MA

11 <sup>7</sup>Oak Ridge Institute for Science and Education, Oak Ridge, TN

12 <sup>8</sup>Meemir Consulting, Durham, NC

13 <sup>§</sup>These authors contributed equally to this work

14 <sup>\*</sup>Corresponding author: Yu-Mei Tan

15

16 Highlights

- 17 • Computational models were used to evaluate methods for exposure reconstruction.
- 18 • Critical data needs were identified in interpreting urinary biomarkers.
- 19 • Recommendations were provided for future biomonitoring studies.

20

21 Keywords: Exposure reconstruction, Biomarker interpretation, Pharmacokinetic modeling,  
22 Physiologically Based Pharmacokinetic Model, Carbaryl, Markov Chain Monte Carlo, Discretized  
23 Bayesian, Exposure Conversion Factor, CARES, Population-based Biomonitoring.

24

25

26 *Disclaimer: The United States Environmental Protection Agency has provided administrative*  
27 *review and has approved the paper for publication. The views expressed in this paper are those of*  
28 *the authors and do not necessarily reflect the views of policies of the United States Environmental*  
29 *Protection Agency.*

## ABSTRACT

30  
31 Sources of uncertainty involved in exposure reconstruction for short half-life chemicals were  
32 characterized using computational models that link external exposures to biomarkers. Using  
33 carbaryl as an example, an exposure model, the Cumulative and Aggregate Risk Evaluation  
34 System (CARES), was used to generate time-concentration profiles for 500 virtual individuals  
35 exposed to carbaryl. These exposure profiles were used as inputs into a physiologically based  
36 pharmacokinetic (PBPK) model to predict urinary biomarker concentrations. These matching  
37 dietary intake levels and biomarker concentrations were used to (1) compare three reverse  
38 dosimetry approaches based on their ability to predict the central tendency of the intake dose  
39 distribution; and (2) identify parameters necessary for a more accurate exposure reconstruction.  
40 This study illustrates the trade-offs between using non-iterative reverse dosimetry methods that are  
41 fast, less precise and iterative methods that are slow, more precise. This study also intimates the  
42 necessity of including urine flow rate and elapsed time between last dose and urine sampling as  
43 part of the biomarker sampling collection for better interpretation of urinary biomarker data of short  
44 biological half-life chemicals. Resolution of these critical data gaps can allow exposure  
45 reconstruction methods to better predict population-level intake doses from large biomonitoring  
46 studies.

47

48

49

## 1.1 INTRODUCTION

50

51 Biomonitoring is a relatively efficient and cost-effective means in which to measure compounds or  
52 their metabolites in blood, urine, or other specimen samples (CDC, 2009a; NRC, 2012).

53 Biomonitoring is often used to track changes in exposures over time or to establish reference  
54 ranges for different population cohorts (e.g., gender, lifestage). Biomarkers measured in  
55 biomonitoring studies may also support risk assessment when integrated with complementary data  
56 on epidemiology, toxicity, exposure, and pharmacokinetics (NRC, 2006). One of the approaches  
57 for using biomarkers in risk assessment is to convert measured concentrations into intake doses  
58 (i.e., reverse dosimetry) for comparison against exposure guidance values already demonstrating  
59 risk connotation, such as the Environmental Protection Agency's (EPA) Reference Dose (RfD)  
60 (NRC, 2006).

61 Reverse dosimetry, however, is not a straightforward process. Cross-sectional biomonitoring  
62 studies such as the CDC's National Health and Nutrition Examination Survey (NHANES) (CDC,  
63 2009a) involve taking a single spot measurement for each individual. Spot measurements reflect  
64 many interacting variables, such as timing of sample collection, as well as exposure sources,  
65 routes, magnitude, duration, and frequency. Spot measurements also reflect the variability  
66 inherent in human pharmacokinetics, namely absorption, distribution, metabolism, and excretion  
67 (ADME) of a chemical in the body. Collection of such information regarding these interacting  
68 variables, and its integration using physiologically based pharmacokinetic (PBPK) models, can aid  
69 in obtaining reasonable estimates for exposures based on biomarker data.

70 PBPK models can predict the time course of a chemical's and its metabolites' (if applicable)  
71 concentrations in biological tissues under various exposure and pharmacokinetic scenarios.  
72 Several research groups have demonstrated the utility of PBPK models in conducting reverse  
73 dosimetry (Allen et al., 2007; Ellison et al., 2012; Liao et al., 2007; McNally et al., 2012; Tan et al.,

74 2006a; Tan et al., 2006b; Ulaszewska et al., 2012). Reverse dosimetry has also been conducted  
75 using simpler pharmacokinetic (PK) models (Lorber, 2009; Lu and Andres, 2012), ratio calculations  
76 (Bartels et al., 2012) methods (Georgopoulos, 1994; Roy and Georgopoulos, 1998), or Bayesian  
77 approaches (Allen et al., 2007; Sohn et al., 2004).

78 Despite the large body of literature associated with using reverse dosimetry to estimate exposure  
79 concentration from biomarker data, efforts for evaluating such predictions have been hampered by  
80 the lack of corresponding measurements of biomarker data with “true” exposure conditions  
81 (Clewell et al., 2008). Exposure reconstruction is challenged by the need for inferring exposures  
82 from extremely limited information commonly gathered in large-scale biomonitoring studies (e.g.,  
83 biomarker data, body weight, and urine volume) for individuals. The objective evaluation of the  
84 appropriateness of different reverse dosimetry methods, influencing determinants of dose-  
85 biomarker relationship, and errors in reconstructed dose estimates is difficult in the absence of  
86 matched exposure/biomarker measurements. As with prior exposure-dose modeling approaches  
87 (Knaak James et al., 2012), the current study utilized a combined exposure-PBPK model for  
88 carbaryl to generate corresponding time profiles of dietary intake doses and urinary biomarker  
89 concentrations in a virtual population. Exposure-dose modeling approach has been previously  
90 applied to investigate health impacts from dermal dietary exposures to an organophosphate  
91 pesticide in members of general population (Ellison et al., 2012; Hinderliter et al., 2011; Price et al.,  
92 2011). In this current study, exposure-dose modeling is used to examine sources of variability in  
93 biomarkers of exposure and identify critical data gaps that might render the ability to reconstruct  
94 intake doses from biomarker data difficult. Our proposed approach can be applied to models for a  
95 wide variety of chemicals, and here carbaryl was selected as a case study to demonstrate the  
96 approach.

97 Carbaryl is a widely used carbamate insecticide with a relatively short biological half-life of 9 hours  
98 (Feldmann and Maibach, 1974), whose routes of exposure include oral ingestion (via food and

99 water), as well as inhalation and dermal contact during application (Howard, 1991). The major  
100 metabolite 1-naphthol (1-N) is found in the urine of exposed individuals and is commonly used as a  
101 biomarker for carbaryl exposure (CDC, 2009b; Meeker et al., 2007). PBPK models for carbaryl in  
102 rats and humans have previously been developed (Nong et al., 2008; Yoon et al., 2015; Yoon et  
103 al., 2012) to predict the disposition of both carbaryl and 1-N. In addition, within-day exposure  
104 profiles (magnitude, frequency, and duration) for food and water exposure from the use of carbaryl  
105 is available from the Cumulative and Aggregate Risk Evaluation System (CARES) (ILSI, 2009)  
106 making carbaryl an ideal candidate for a case study to compare reverse dosimetry approaches and  
107 to investigate critical data needs. The two objectives of this study were to: (1) compare three  
108 PBPK model-based reverse dosimetry approaches based on their ability to predict the central  
109 tendency of the intake dose distribution; and (2) identify information necessary for a more accurate  
110 dose intake estimate from biomarker data of short biological half-life chemicals.

## METHODS

111

### 112 *Estimating dietary exposures to carbaryl using CARES*

113 A dietary exposure model, the Cumulative and Aggregate Risk Evaluation System (CARES)  
114 Version 3.0 (ILSI, 2009), was used to estimate carbaryl exposure from food and water  
115 consumption. The CARES model has been formally reviewed and approved by the EPA's Science  
116 Advisory Panel (USEPA, 2004) and has been used by the EPA's Office of Pesticide Programs  
117 (USEPA, 2006a; USEPA, 2006b; USEPA, 2007) to estimate carbaryl intake in the general  
118 population. The CARES model combines data on food and water consumption with data on  
119 pesticide residues, such as carbaryl, in order to characterize variation in total dietary exposure in  
120 the U.S. population. CARES produces sequential estimates for periods of up to one year with a  
121 resolution of 10 minutes. CARES uses the Gower's Similarity Coefficient to identify demographic  
122 and anthropometric records that correspond to individuals with statistically similar characteristics,  
123 such as gender and age. Using this technique, year-long (365 days) dietary profiles (time-dose  
124 relationships of carbaryl exposures) were constructed for a set of simulated individuals (n=500)  
125 (Crop-Life-America, 2002).

126 Dietary exposure from food and water was determined based on consumption data from the  
127 Continuing Survey of food Intake by Individuals (CSFII) from 1994-1996, and 1998 (USDA, 2000).  
128 The nationwide survey indicates the time of day a food and/or meal was consumed which allows  
129 the exposure to be characterized by each meal or eating event. To allow the CSFII food  
130 consumption data to be expressed as raw agricultural commodities (RACs) or processed  
131 commodities, the Food Commodity Intake Database (FCID) was used to provide translation  
132 recipes (USEPA and USDA, 2000). Additionally, the CSFII database contains water consumption  
133 data for indirect water (i.e., water added to foods and beverages during final preparation), and for  
134 water consumed directly. A nationally representative water consumption survey has been

135 conducted to address how often, when, and how much water is consumed at specific times during  
136 the day (Barraj et al., 2009). These data were incorporated into CARES to give the time of day  
137 information for water consumption.

### 138 ***Simulating spot urinary 1-N concentrations using a PBPK model***

139 A human PBPK model for carbaryl (Yoon et al., 2012) was used to predict the disposition of the  
140 parent chemical (i.e., carbaryl, the active species for acetyl cholinesterase [AChE] inhibition) and  
141 the principal metabolite and primary biomarker used to indicate carbaryl exposure, 1-N. The  
142 model was parameterized using human-specific *in vitro*-derived metabolic constants of carbaryl in  
143 combination with knowledge gained from modeling carbaryl kinetics and responses in the rat (see  
144 parameters used for the PBPK model in Supplementary Table 1). The PBPK model predicts the  
145 urinary concentration of total 1-N (free, plus conjugates) as reported in biomonitoring studies. For  
146 each of the 500 CARES individuals, the synthetic daily intake doses were added directly into the  
147 gut compartment of the PBPK model.

### 148 ***Sensitivity Analysis of the PBPK model***

149 A local sensitivity analysis was conducted to identify PBPK parameters with the greatest influence  
150 on predicted 1-N urinary concentrations. Seven days were sufficient for the model-predicted  
151 urinary 1-N excretion to reach pseudo steady state. Three dose levels were tested: the 5<sup>th</sup>  
152 percentile, the 50<sup>th</sup> percentile, and the 95<sup>th</sup> percentile of the distribution of the largest single dose  
153 per day for all individuals (N = 365 days × 500 individuals = 182,500). These doses were 0.7359,  
154 35.09, and 154.9 ng carbaryl/kg body weight/day, respectively. The elapsed time between the final  
155 dose at each level and the time of urine sampling was also fixed at one of three values: 1, 4, or 12  
156 h. In summary, a sensitivity analysis of all model parameters was performed for nine separate  
157 cases, with each case being a unique combination of dose level and the elapsed time between  
158 dosing and urine sampling. Model parameters (other than the one undergoing sensitivity analysis)

159 were set to their mean values (either the arithmetic mean or geometric mean, depending on the  
160 shape of the distribution for that variable). Normalized sensitivity coefficients were computed by  
161 dividing the change in the urinary 1-N concentration by the change in the parameter value after  
162 perturbing the value by 0.1% of its mean. Sensitive parameters were considered to be those with  
163 normalized sensitivity coefficients  $\geq 0.1$ .

#### 164 ***Generating the Synthetic Data for Paired Intakes and Biomarkers***

165 Since reconstructing intermittent doses at random times from a single spot urine biomarker  
166 measurement proves difficult, the food and water exposure profiles simulated in the CARES model  
167 required simplification using two assumptions to generate synthetic daily intake doses:

168 (1) Each of the 500 individuals received one dose per day, for 5 days. This daily dose was the  
169 mean of 365 daily intake doses (sum of all intermittent doses within a 24 h period) from the  
170 CARES simulations, which will henceforth be referred to as the synthetic daily intake  
171 doses.

172 (2) Each individual received a single daily dose at the same time each day (2:42 pm) in order  
173 to consistently simulate daily intake of contaminated food or water. The time of exposure  
174 was the median of 365 time points at which the maximum dose occurred, unique to each  
175 individual.

176  
177 Each of the 500 CARES individuals was assigned a unique vector of parameter values: body  
178 weight (kg) was taken from the CARES model (range from 35.6 kg to 158.8 kg, with an average of  
179 74 kg), and sensitive parameters (results in Supplementary Table 2) were randomly chosen from  
180 their distributions (see Supplementary Table 1). These distributions were truncated at  $\pm 1.96 \times \sigma$ ,  
181 where  $\sigma$  is the standard deviation. This truncation limited sampling to approximately the central  
182 95% of the total distribution and prevented extreme values from being sampled. All non-sensitive

183 model parameters were fixed to their mean (see Supplementary Table 1). This vector of sensitive  
184 and non-sensitive parameters is henceforth referred to as individual values for the synthetic  
185 individuals (known parameter values). The model was then used to predict the rate of production  
186 of 1-N in urine,  $r(t)$  (ng/h) as a function of time for each individual.

187 The model output, as a rate, required conversion to a spot urinary concentration (e.g., in ng/L), the  
188 units typically reported in biomonitoring studies. This conversion was accomplished through the  
189 use of two equations. The first equation used urine volume and the time between voids:

190 Equation 1: 
$$c(t_s) = \frac{1}{V_u} \int_{t_{s-1}}^{t_s} r(t) dt = \frac{1}{V_u} [m(t_s) - m(t_{s-1})],$$

191 where  $c(t)$  is the concentration of 1-N in urine (ng/L) at time  $t$ ,  $V_u$  is the volume of the urine void  
192 (L),  $t_s$  is the time of sampling (h),  $t_{s-1}$  is the time of the most recent urine void before the sampling  
193 time (h),  $r(t)$  is the mass flow rate of 1-N into the urine (ng/h), and  $m(t)$  is the cumulative amount  
194 (ng) of 1-N in urine.

195 An alternative equation based on urine flow rate calculated the quantity of urine produced in a  
196 specified period of time.

197 Equation 2: 
$$c(t_s) = \left( \frac{r(t_s)}{fr} \right),$$

198 where  $fr$  is the urine flow rate (L/h).

199 For this study, values for urine volumes, time between voids, and urine flow rates were obtained  
200 from the NHANES 2009-2010 dataset (CDC, 2011). The two methods for calculating the urine  
201 concentration from the model output were compared (See Table 1 for simulation description  
202 summary). It was found that the predicted spot urinary 1-N concentrations using both equations  
203 were nearly identical (see Supplementary Figure 1). Thus, the second equation, which required  
204 only one additional parameter (urine flow rate) rather than two parameters (urine volume and time

205 between voids), was used to compute spot urinary 1-N concentrations for the synthetic individuals.  
206 For each of the 500 CARES individuals, urine flow rate was randomly sampled from the NHANES  
207 2009-1010 dataset.

208 The elapsed time between the final dose and spot urine sampling was constrained to be no more  
209 than 24 h. The NHANES dataset includes a “sampling session” variable, which was used to assist  
210 in setting the time of spot urine sampling. These sampling times were designated as occurring in  
211 the morning (8:00 am – 12:30 pm), afternoon (1:30 – 5:30 pm), or evening (5:30 – 9:30 pm). The  
212 exact sampling time for each individual is kept confidential in NHANES, so a time was randomly  
213 assigned in our study from a uniform distribution in one of the sampling session windows. Based  
214 on NHANES data collected between 1999 and 2010, 46.7% of simulated individuals were sampled  
215 in the morning, 35.7% in the afternoon, and 17.7% in the evening (see Supplementary Table 3).  
216 Since the time of daily exposure was fixed for each simulated individual, some biomarkers for  
217 some were sampled on the 5<sup>th</sup> day after the 5<sup>th</sup> dose, while biomarkers for others were sampled on  
218 the 5<sup>th</sup> day between the 4<sup>th</sup> and 5<sup>th</sup> dose.

219 In summary, each of the 500 CARES individuals were assigned values for the following variables:  
220 a fixed daily dose of carbaryl which was the mean of his/her 365 CARES-simulated daily doses; a  
221 fixed time of exposure which was the mean of his/her 365 CARES-simulated time at which  
222 maximum dose occurred; a urine flow rate randomly sampled from NHANES 2009-2010; and a  
223 spot urine sampling time on the 5<sup>th</sup> day, randomly sampled from a distribution generated based on  
224 NHANES sampling sessions. Next, using the PBPK model, a corresponding urinary 1-N  
225 concentration (CARES-predicted intake doses, PBPK-predicted urinary 1-N concentrations, and  
226 model parameter values are listed in Supplementary Table 4) was predicted using these inputs  
227 (see Supplementary Figure 1, Eq. 2, red dotted histograms). These data were used in the  
228 subsequent analyses to compare three reverse dosimetry approaches. The synthetic daily intake  
229 doses were fit to a log-normal distribution for ease of comparison to population distribution

230 estimates generated by reverse dosimetry approaches. All simulations described in this article are  
231 summarized in Table 1.

232

233

### 234 ***Comparing three reverse dosimetry approaches***

235 In the current study, three PBPK model-based reverse dosimetry approaches were evaluated:  
236 Exposure Conversion Factor (ECF), Discretized Bayesian (DBA), and Markov Chain Monte Carlo  
237 (MCMC) (Georgopoulos et al., 2009; Tan et al., 2006a). For all three methods, the only “unknown”  
238 parameter estimated from the urinary 1-N concentrations was daily intake dose. All other model  
239 parameters were kept the same for the synthetic individuals, using each method. Daily intake  
240 doses estimated from these three methods were compared to the synthetic daily intake doses.

241 The ECF method required a Monte Carlo (MC) simulation of the PBPK/PD model, given a unit  
242 dose of carbaryl (1 ng/kg/day) (Liao et al., 2007; Tan et al., 2006a; Tan et al., 2006b). In this  
243 analysis, however, MC randomization was not performed since the only “unknown” was the intake  
244 dose. Rather, a distribution of 500 urinary 1-N concentrations was generated by running the PBPK  
245 model using the same parameter values as those generated from the synthetic data, given a unit  
246 dose of carbaryl. Next, the reciprocal of the distribution of predicted urinary 1-N concentrations

247 (generated from the unit dose) was calculated as the ECF distribution, in units of  $\frac{\text{ng carbaryl}}{\text{kg body weight}} \bigg/ \frac{\text{ng 1-N}}{\text{L urine}}$

248 The ECF distribution was then convolved with the distribution of synthetic urinary 1-N  
249 concentrations to obtain an estimate of the distribution of daily intake doses of carbaryl. The ECF  
250 method is only applicable when the dose-biomarker relationship is linear. The other two methods  
251 (DBA and MCMC) do not require this assumption.

252 The DBA method was based on Bayes' formula (Liao et al., 2007; Tan et al., 2006a):

253 Equation 3:  $(C_j|N) = \frac{P(N|C_j)P(C_j)}{\sum_i P(N|C_i)P(C_i)}$ , for  $i,j= 1,2, \dots , T$

254 where  $C$  is the intake dose of carbaryl,  $N$  is the urinary 1-N concentration,  $P(C_j|N)$  is the probability  
255 of a carbaryl intake concentration,  $C_j$ , given an observed urinary 1-N concentration,  $N$ ;  $P(C_j)$  is the  
256 prior distribution for the discrete carbaryl doses,  $C_j$ ; and  $P(N|C_j)$  is the probability of a urinary 1-N  
257 concentration,  $N$  (predicted by a model that describes the dose-biomarker relationship), given a  
258 carbaryl dose,  $C_j$ .  $T$  is the total number of discrete carbaryl doses  $C_j$  and corresponding predicted  
259 urinary 1-N concentrations,  $N_j$ .

260 The ability to specify a prior distribution for exposure concentrations and to handle a non-linear  
261 dose-biomarker relationship differentiates the DBA from the ECF method. A MC simulation was  
262 run for each of the  $T$  discrete exposure doses to generate distributions of  $P(N|C_j)$ . The prior  
263 exposure concentrations,  $C_j$ , were selected to cover the range of possible doses and the non-  
264 linear range of the dose-biomarker relationship. This matrix for  $P(N|C)$  involved rows  
265 corresponding to the number of exposure concentrations tested ( $T$ ) and columns corresponding to  
266 the number of MC iterations. The matrix for  $P(N|C)$  was then transformed into the posterior,  
267  $P(C|N)$  using the equation above. The transformed matrix was then multiplied by the distribution of  
268 observed biomarker concentrations,  $P(N_{obs})$ , to obtain the estimated distribution of carbaryl  
269 exposure for the population,  $P(C)$ , according to Equation 4.

270 Equation 4:  $P(C) = P(C|N) \times P(N_{obs})$ .

271 In our analysis, the discrete carbaryl daily doses ranged from  $10^{-2}$  ng/kg/day to  $10^6$  ng/kg/day, with  
272 increments on a  $\log_{10}$ -scale by  $10^{0.08}$  ( $T=101$ ). This range was chosen based on the result of the  
273 ECF method, after adding a buffer of one order of magnitude. Both ECF and DBA are  
274 deterministic methods. Parameter values for each of the 500 CARES individuals were used to  
275 generate a predicted urinary 1-N concentration at a given dose. The total number of simulations

276 for the DBA method was 500 parameter sets  $\times$  101 unique doses = 50,500 iterations. Two priors  
277 of carbaryl intake  $P(C_j)$  were used:

278 (1) A uniform prior (for each carbaryl intake dose  $C_j$ , the probability was the same,  $[10^{-2}, 10^6]$   
279 ng/kg/day), and

280 (2) A biased prior (a normalized lognormal distribution with a geometric mean of  $1 \times 10^3$  ng/kg/day  
281 and a geometric standard deviation of  $\sqrt{10}$ , and the prior was truncated at 1 ng/kg/day and  $10^6$   
282 ng/kg/day).

283 The first prior was chosen to represent a non-informative case, in which only the bounds on intake  
284 doses were suggested. The second prior was chosen to represent a situation in which supporting  
285 data provided a reasonable mean exposure value; this second prior was approximated by a  
286 lognormal distribution with a large standard deviation to capture uncertainty. Even when a prior is  
287 supported, it may impose bias as it relates to the biomonitoring data used in reverse dosimetry.  
288 We wished to observe whether DBA could correct for this bias in the prior. Both ECF and DBA  
289 methods were executed using the web-based tool, PROCEED (Grulke et al., 2013)  
290 <http://www.epa.gov/heasd/research/proceed.html>).

291 The MCMC approach used an iterative application of Bayes' theorem, with the distributions  
292 regarded as continuous rather than discrete (McNally et al., 2012; Ulaszewska et al., 2012). In  
293 other words, MCMC was not confined to the range of exposure values given in the priors, in  
294 contrast to what was seen in the case of the DBA method. Specifically,  $P(C|N) \propto P(C)P(N|C)$ ,  
295 where  $P(C)$  is the prior distribution for intake doses of carbaryl,  $P(N|C)$  is the likelihood function,  
296 and  $P(C|N)$  is the posterior distribution of the carbaryl exposure given the observed urinary 1-N  
297 concentrations. MCMC algorithms stochastically approximate the joint-posterior distributions  
298 without having to sample the entire space and were particularly well-suited for solving non-linear  
299 inverse problems. In this study, the deterministic PBPK model was configured to run with the

300 population means and standard deviations for its kinetic and metabolic parameters (see  
301 Supplementary Table 1). The priors for the population mean intake were set based on a  
302 normalized lognormal distribution with a geometric mean  $\mu_C = 100$  ng/kg/day and geometric  
303 standard deviation of 200, truncated at  $10^{-4}$  ng/kg/day and  $1 \times 10^5$  ng/kg/day. The priors for the  
304 population variance were set based on a normal distribution with a mean  $\mu_C = 100$  ng/kg/day and  
305 standard deviation of 50 ng/kg/day, truncated at  $10^{-4}$  ng/kg/day and  $10^3$  ng/kg/day. These priors  
306 were based on the results from the ECF and DBA methods (DBA: uniform prior) since both  
307 methods had similar distributions and a large standard deviation. The function,  $N=f(C)$ , represents  
308 the PBPK model for carbaryl using dose,  $C$  (ng/kg/day), as input and 1-N concentrations in urine,  
309  $N$  (ng/L), as output. The input, “ $C$ ”, was inferred by estimating the distributions of population mean  
310 and variance (Bois, 2000) using AcslX (The AEGIS Technologies Groups, Inc., Huntsville, AL). It is  
311 a common practice to remove the burn-in from the resulting chains, and thus, the first 7,000  
312 iterations were removed in our analysis. Fifty sets of mean and variance were selected from the  
313 MCMC output chains to generate 50 possible distributions of “ $C$ ”, and then 500 values were  
314 randomly selected from each of the 50 distributions to obtain 25,000 “ $C$ ” possibilities, which  
315 contributed to the final estimates of the distribution of “ $C$ ”.

316

### 317 ***Evaluating the value of information in exposure reconstruction***

318 The approach presented above allowed us to evaluate the efficiency of different reverse dosimetry  
319 methods in reconstruction of daily intake doses when these doses were the only unknown (referred  
320 to as “all parameters known”). The impact of missing information in exposure reconstruction was  
321 evaluated by (1) setting all parameter values to their means, (2) setting individual parameter values  
322 to either (2) their *known* value, or (3) a random value from population distributions supported by  
323 literature. The parameters we tested in this analysis were: (1) elapsed time between the final

324 dose and urine biomarker sampling (potentially measurable), (2) urine flow rate (potentially  
325 measurable), and (3) urinary elimination rate of 1-N and its metabolites (the most sensitive  
326 parameter from the local sensitivity analysis, but not directly measurable in humans).

327 A common practice for reconstructing daily intake doses based on real-world biomarker data  
328 involves setting model parameters to their respective means, which is assumed to result in  
329 reasonable estimates in the absence of measured data. Thus, in this first analysis (Case 1),  
330 certain model parameters of interest were replaced with their respective means.

331 Case 1 (Means): All of the parameters being tested were set to their means.

332 (1) The elapsed time between the final dose and urine sampling was set to -0.865  
333 hours (after the fourth day's dose, but just before the fifth day's dose). This was  
334 the mean from our 500 synthetic individuals.

335 (2) The urine flow rate was set to 0.6526 mL/min based on the mean of NHANES  
336 2009-2010 (CDC, 2011) .

337 (3) The most sensitive PBPK parameter, the urinary elimination rate was set to its  
338 mean,  $0.2/\text{h}/\text{kg}^{-1/4}$  (Yoon et al., 2012).

339 The MCMC method, with the same priors as described above, was used to reconstruct daily intake  
340 doses to investigate the impact of using population means for all model parameters on  
341 reconstructing population intakes (Case 1).

342 In the next two components of the analysis (Cases 2 and 3), all parameters were set to their mean  
343 values, except for the three parameters mentioned above (e.g., elapsed time between dose and  
344 sampling, urine flow rate, and urine elimination rate). Rather than using the means for all three  
345 parameters as with case 1, two parameters were set to their means one at a time, while the third  
346 was altered as described below for each individual case:

347 Case 2 (Default): The parameter being tested was assigned independently to the synthetic  
348 individual values used to generate the urinary 1-N concentrations. This case corresponds to a  
349 situation in which measurements of the elapsed time, urine flow rate, or urinary elimination rate  
350 are collected as part of a biomonitoring study.

351 Case 3 (Random): The parameter being tested was randomly selected from a distribution:

352 (1) A normal distribution for elapsed time between the final dose and urine sampling,  
353  $t_{elapsed} \sim N(-.86523, 6)$ , in hours. This distribution was obtained from the synthetic  
354 individuals, with a wider standard deviation to account for uncertainty.

355 (2) A lognormal distribution for the urine flow rate with a geometric mean of 0.6526 mL/min  
356 and a geometric standard deviation of  $\sqrt{10}$ . This distribution was obtained from  
357 NHANES 2009-2010 (CDC, 2011) , with a wider standard deviation to account for  
358 uncertainty.

359 (3) A lognormal distribution for the urinary elimination rate of 1-N, with a geometric mean of  
360  $0.2/h/kg^{-1/4}$  and a geometric standard deviation of 1. This distribution was obtained from  
361 the literature based on animal values (Knaak, 1968; May et al., 1992; Yoon et al.,  
362 2012), with a wider standard deviation to account for uncertainty.

363 Case 3 is similar to setting all parameter values to their respective means (Case 1); however,  
364 the parameter distribution was inferred from other information in addition to the mean values.  
365 For example, the exact time of exposure events may not be recorded in the biomonitoring  
366 study, but the general time frame for sampling collection might be known (e.g., between 9 am  
367 and 5 pm). Or, urine flow rate may be estimated from a carefully measured urine void volume  
368 and self-reported time between voids, which were subject to uncertainty inherent in human  
369 recalls. Or, a distribution of urinary elimination rate of 1-N may be obtained from the literature  
370 since this parameter is only measurable in animals.

371 As described earlier, the burn-in of 7,000 iterations were removed in all cases, except when  
372 examining the influence of urinary elimination rate. Because the Markov chain converged faster  
373 when updating urinary elimination rate, only the first 3,000 iterations were removed. These six  
374 additional trials (from Cases 2 and 3: 3 parameters  $\times$  2 cases) aided in the evaluation of the value  
375 of incorporating additional information for specific parameters, using the MCMC method. A  
376 summary of the different simulations and analyses described above is given in Table 1.

377 A Welch t-test was conducted to determine if the means of each of the MCMC posterior  
378 distributions of intakes were significant different than the mean of the CARES-synthetic intake  
379 distribution. This test was repeated for each of the MCMC simulations.

380

381

382

## RESULTS

383 The CARES model was used to estimate daily carbaryl intake doses for 500 simulated individuals,  
384 which were then fit to a log-normal distribution (Figure 1). These synthetic intake doses were then  
385 compared against other “reconstructed doses” (Tables 2 and 3). The CARES-synthetic geometric  
386 mean was 70 ng/kg/day, and the geometric SD was 4.1 (Table 2). Comparison of the population  
387 distribution estimates of carbaryl daily intake doses from the three reverse dosimetry methods with  
388 the distribution of the CARES- synthetic daily intake doses showed that all three methods were  
389 reasonably good at estimating the mean of the distribution (Table 2). The estimated geometric  
390 mean daily intake was 97, 100, 251, and 92 ng/kg/day for the ECF, the DBA (uniform prior), the  
391 DBA (biased prior) and MCMC, respectively (Table 2). The mean intake doses estimated by the  
392 three reverse dosimetry methods (ECF, DBA: uniform prior, and MCMC) were more similar to each  
393 other than to the mean CARES-simulated dose, and all three methods overestimated the mean  
394 intake dose (Table 2). The ECF and the DBA (both priors) methods provided similar estimates of  
395 the population SD, but both these estimates were significantly larger (about 200 times) than the  
396 CARES-synthetic SD. On the other hand, the MCMC-estimated geometric SD was 4.5, which was  
397 fairly similar to the CARES-synthetic geometric SD. Thus, out of the three reverse dosimetry  
398 methods, MCMC performed the best in our dose reconstruction analysis.

399 Comparing the posterior distributions obtained from two different priors in the DBA method, the  
400 posterior mean updated from the uniform prior was more similar to the population geometric mean  
401 of the CARES-synthetic intake doses (Figure 2a, black line vs blue dashed-dotted line). While the  
402 posterior mean updated from the non-uniform (biased) prior remained biased (Fig 2b. black line vs  
403 blue dashed-dotted line), the posterior mean was improved compared to its prior (Fig 2b, black line  
404 vs red dotted line). Additionally, the posterior distribution updated from the non-uniform prior was  
405 tighter and more precise, though less accurate, than that updated from the uniform prior (Figure 2).

406 Next, the impact of missing information was evaluated. The MCMC analysis from the method  
407 comparison was included for purposes of comparison. The distribution generated assuming “all  
408 parameter values are known” had a GM of 92 ng/kg/day, and a GSD of 4.5; while the distribution  
409 generated by “setting all parameter values to their respective means” (case 1) had a geometric  
410 mean of 47 ng/kg/day, and the geometric SD was 0.8 (Table 3).

411 For five of the six MCMC trials, the inferred GM (ranging from 352 to 690 ng/kg/day) overestimated  
412 the CARES-synthetic GM (70 ng/kg/day) by one order of magnitude (Table 3). The only exception  
413 was for the case in which urine flow rates were randomly selected from a distribution (Table 3,  
414 “Urine Flow Rate, MCMC-random”). In this case, the geometric mean, 45,968 ng/kg/day, was  
415 three orders of magnitude greater than that of the CARES-synthetic daily intake doses (Table 3).  
416 All six MCMC trials overestimated the geometric SD (ranging from 59 to 30,055). Again, the “Urine  
417 Flow Rate, MCMC-random” case resulted in the largest estimate of the geometric SD (Table 3).

418 Intake doses in the “Urinary Elimination Rate, MCMC-default” and the Urinary Elimination Rate,  
419 MCMC-random” cases were similar to each other, with slightly less error in the MCMC-random  
420 case (Table 3). Estimated intake doses for the elapsed time and urine flow rate, MCMC-random  
421 cases showed a larger geometric mean/SD than did intake doses in the MCMC-default cases for  
422 both parameters (Table 3). However, the performance of the dose reconstruction was extreme in  
423 both cases for urine flow rate. MCMC-default (Case 2: urine flow rate) performed the best among  
424 the six cases, while the MCMC-random (Case 3: urine flow rate) performed the worst among the  
425 six cases (Table 3). This finding indicates that knowledge of urine flow rate is critical when  
426 attempting to reconstruct doses based on urine metabolites of short half-life chemicals.

427 A Welch’s t-test revealed that the means of each of seven out of the eight MCMC distributions  
428 were significantly different (0.05 level) from the mean of the CARES-synthetic distribution (Table

429 3). When all parameters were set to their means (Case 1) the mean of the MCMC distribution was  
430 not significantly different than the mean of the CARES-synthetic distribution.

431

## DISCUSSION

432 In their publication "*Exposure Science in the 21<sup>st</sup> Century*", the National Research Council reported  
433 that biomarker data "will be essential for evaluating the efficacy of exposure reduction policies, and  
434 for prioritizing and assessing chemical risks" (NRC, 2012). One way to achieve these goals is to  
435 convert biomarker data to intake doses for comparison to an established exposure guidance value.  
436 Exposure guidance values are usually determined through animal toxicity studies, in which  
437 administered target tissue doses are known and measurable. In humans, however, most target  
438 organs cannot be examined, and often only biomarkers in accessible media can be collected. Due  
439 to the difficulty in directly associating biomarker measurements with target tissue doses, the  
440 common approach for biomarker use in risk assessment is conversion of its concentration to an  
441 exposure level. One basic assumption that is often ignored with this approach is that the  
442 biomarker should have a strong, direct correlation with intake doses (LaKind et al., 2014). In cases  
443 where the biomarker is a poor surrogate of intake doses, which often occurs for short half-life  
444 chemicals, these biomarker measurements are only suitable for trend analysis (e.g. do biomarker  
445 concentrations change with time?) or comparison among different groups (e.g. male/female).

446 In the current study, the ability of three different reverse dosimetry approaches to reconstruct  
447 intake doses was investigated using model-simulated data. Corresponding intake doses,  
448 physiological measurements, and pharmacokinetic data are rarely collected in conjunction with  
449 biomarker measurements. Thus, the most viable approach is to generate "unmeasured" data  
450 using models (Georgopoulos et al., 2009; Phillips et al., 2014a; Phillips et al., 2014b). For  
451 example, Georgopoulos et al., (2009) also compared the performance of the ECF and the DBA  
452 models using actual biomarker data with known exposure data or "synthetically augmented" data  
453 (i.e., missing information was filled using randomly sampled values from distributions) and found  
454 that reconstruction using the synthetic data better facilitated the evaluation of reverse dosimetry  
455 methods and characterization of the value of additional information.

456 In our study, comparison of the three reverse dosimetry approaches in reconstruction of intake  
457 doses based on urinary biomarkers suggests that MCMC exhibited the best capability at identifying  
458 the population variance. The use of the MCMC, however, requires increased computational  
459 resources compared to the other two methods explored in this study. Seventy-two hours was  
460 necessary for the completion of a hierarchical analysis on a quad-core 2.2 GHz i7 MacBook, while  
461 only minutes were necessary for completion of the ECF and the DBA models using PROCEED  
462 (Grulke et al., 2013). Further computational/runtime improvements may be possible if the  
463 population size was reduced from 500 individuals, as the number of simulation runs required per  
464 MCMC iteration scales with the number of individuals. Such reduction, however, is unlikely to be  
465 realistic when interpreting biomarker results from large-scale studies, such as NHANES.

466 Other reverse dosimetry approaches that are not evaluated in the current study, such as  
467 optimization or trial-and-error approach (Mosquin et al., 2009; Roy and Georgopoulos, 1998) and  
468 “multiplier” (e.g., fraction of total dose in urine) can back-calculate intake doses from biomarker  
469 data (Lakind and Naiman, 2008; Lorber et al., 2011; Payne-Sturges et al., 2009). The  
470 performance of the “multiplier” approach depends solely upon the accuracy of the “multiplier”, and  
471 the performance of the optimization approach is highly related to the optimization routine selected.  
472 Bayesian approaches, such as the DBA method examined in the current study, can also be  
473 implemented as an optimization scheme.

474 Given that the MCMC method exhibited the ability to closely infer the population mean and  
475 variance of synthetic daily carbaryl intakes simulated from CARES, this modeling approach was  
476 also used to evaluate the impact on reconstructed doses from uncertainty in specific parameters.  
477 Case 1, which is the only MCMC case that estimated a population mean not significantly different  
478 from the CARES-synthetic mean, is analogous to representing the entire population using an  
479 “average individual”. Thus, the estimated average intake dose adequately reflects the CARES  
480 average synthetic intake dose. This finding is consistent with the general agreement that the

481 central tendency of the distribution of biomarker concentrations is to reflect long-term average  
482 exposures in a population (Aylward et al., 2012; Pleil and Sobus, 2013; Rao et al., 2012). Since  
483 the only variability in this case came from urinary 1-N (biomarker) concentrations (all parameters  
484 were set to their means), the estimated SD was the smallest among all cases.

485 The MCMC case in which all parameter values were “known” and independently assigned for  
486 individuals would have been expected to provide the best estimates of intake dose. While the  
487 estimated mean from this case slightly overestimated the CARES-synthetic mean, this MCMC  
488 case did provide the best estimate of the overall distribution (Table 3). In addition to the variability  
489 in urinary 1-N concentrations, this MCMC case also included the variability in PBPK parameters,  
490 urine flow rate, and time of urine sampling. The inclusion of these parameter values provided  
491 sufficient information for updating the intake estimates. As a result, this MCMC case was able to  
492 predict a similar variance as the CARES-synthetic distribution.

493 In our simulation study, the value for each parameter was known, which made the MCMC-default  
494 case possible (MCMC from method comparison, and Case 2). In real life, however, it is not often  
495 feasible to collect a specific piece of information from each individual in a population. In some  
496 cases, certain data (e.g., time between urine voids) can be collected as part of the biomonitoring  
497 study if the study designers are aware of these parameters’ importance. Often, information is  
498 available only at the population level, and the value of an unmeasured parameter may be  
499 estimated based on the central tendency of a distribution (set all parameter values to their means)  
500 or the entire distribution for the population (randomly select parameter values from distributions).

501 Out of the three parameters selected for evaluating the impact of missing information in this study,  
502 urine flow rate was the most influential on the performance of the dose reconstruction. Dose  
503 reconstruction using MCMC requires the comparison of model predictions to measured biomarker  
504 data, in this case the concentration of 1-N in urine, to update the intake dose estimates. Urinary 1-

505 N concentration is calculated by dividing the PBPK model-predicted mass flow rate of 1-N into the  
506 urine (ng/h),  $r(t)$ , by the urinary flow rate,  $fr$  (see the flow rate calculation, Eq. 2). In other words, a  
507 single urinary 1-N concentration may be calculated from infinite combinations of model-predicted  
508 1-N excretion rates and urine flow rates (i.e., no unique solution). As a result, MCMC was unable  
509 to estimate a reasonable intake distribution when urine flow rate was allowed to vary (“Urine Flow  
510 Rate, MCMC-random”, Case 3, Table 3). Alternatively, when  $fr$  was assigned using each  
511 individual’s value (“Urine Flow Rate, MCMC-default”, Case 2, Table 3), the reconstructed mean  
512 intake dose was the closest (of the six presented cases) to the CARES-simulated mean despite a  
513 significant difference still existing between the two means. Another study that examined  
514 contributors to biomarker variability, assuming a single dose, also identified variability in urine flow  
515 rate as a major influence compared to variability in other physiological or pharmacokinetic  
516 parameters (Phillips et al., 2014a). In 2009-2010, urine flow rates began being included in the  
517 NHANES sampling data set (CDC, 2011). To accomplish this, volume of urine was collected and  
518 participants were asked to recall the time of their last void. Urine flow rate was obtained by  
519 dividing urine volume by the time between voids. This is a promising step towards fixing data gaps  
520 in the use of biomarker data to understand exposure, although it should be noted that uncertainties  
521 in recollection of void times could still lead to data inaccuracies.

522 The second circumstance in which it proved difficult to predict a parameter value was  
523 demonstrated through the uncertainty in the parameter investigated: elapsed time between the  
524 final dose and the time of urine sampling. For short half-life chemicals, a larger intake dose with  
525 longer elapsed time and a smaller dose with shorter elapsed time may result in the same  
526 biomarker concentrations. Comparing between the two MCMC cases, “Elapsed Time, MCMC-  
527 default” and “Elapsed Time, MCMC-random”, (Cases 2 and 3, respectively, Table 3), the difficulty  
528 of accurately estimating the magnitude of intake doses was demonstrated when the elapsed time  
529 between the final exposure dose and urine sampling is not recorded in a biomonitoring study

530 (Case 3: MCMC-random). Both elapsed time and urine flow rate (or, alternatively, the void volume  
531 and time between voids) are data that can be collected easily. The accuracy of these values can  
532 be greatly improved when the study managers are made aware of importance of recording these  
533 data rather than having the participants recall the information.

534 The third parameter investigated in our study was the urine elimination rate. The estimated intake  
535 doses were similar whether this parameter was set to known values ("Urine Elimination Rate,  
536 MCMC-default", Case 2) or assigned randomly from a distribution ("Urine Elimination Rate,  
537 MCMC-random", Case 3) (Table 3). In other words, randomly sampling from a distribution was  
538 appropriate enough to represent the urine elimination rates for individuals. This finding is  
539 reassuring because urine elimination rate is not measurable in humans, and its distribution may be  
540 obtained from animal studies.

541 We generally found that all of the six cases (MC-default and MCMC-random) overestimated the  
542 population mean and variance of the carbaryl intake doses compared to the MCMC case in which  
543 all parameters were set to their respective means. A likely explanation for this overestimation is  
544 that urine flow rates and urine elimination rates are log-normally distributed. This implies that  
545 values much larger than the geometric mean were included in the MCMC analysis, resulting in  
546 larger estimations of intake doses. While the elapsed time between the final dose and urine  
547 sampling was assumed normally distributed, we did increase the SD of the distribution to account  
548 for uncertainty. As a result, much longer elapsed times were included in the MCMC analysis, also  
549 resulting in higher estimated intake doses.

550

551  
552  
553  
554  
555  
556  
557  
558  
559  
560  
561  
562  
  
563  
  
564  
  
565  
  
566  
567  
568  
569  
570  
  
571  
  
572

## CONCLUSIONS

In conclusion, our study has illustrated the trade-offs between using non-iterative methods for exposure reconstruction (e.g. ECF, and DBA) vs. iterative methods (e.g. MCMC), as well as the impact of uncertainty in specific model parameters in exposure reconstruction methods. This study has demonstrated the importance of including measurements for urine flow rate (or volume of void, and time between voids) and elapsed time between last dose and urine sampling as part of the biomarker sampling collection. Including these measurements in biomonitoring studies will facilitate more accurate exposure reconstruction, allowing for interpreting biomarker data in a risk context. Without these measurements, the uncertainty surrounding exposure estimates may dramatically limit the interpretation of biomarker results. If critical data gaps can be resolved, especially for unidentifiable model parameters, exposure reconstruction methods (e.g. MCMC) can be utilized to better predict population-level intake doses from large biomonitoring studies.

## ACKNOWLEDGEMENTS

The authors would like to thank Yuching Yang at the Hamner Institute for clarifications regarding the human PBPK model for carbaryl. The authors are also grateful to Drs. Rogelio Tornero-Velez, Lisa Baxter, and Roy Fortmann at the EPA for their review and comments. Jingtao Lu and Jeremy Leonard are funded by the Oak Ridge Institute for Science and Education's Research Participation Program at the US-Environmental Protection Agency.

## References

- 573  
574  
575 Allen, B. C., et al., 2007. Use of Markov Chain Monte Carlo Analysis with a Physiologically-Based  
576 Pharmacokinetic Model of Methylmercury to Estimate Exposures in U.S. Women of  
577 Childbearing Age. *Risk Analysis*. 27, 947-959.
- 578 Aylward, L. L., et al., 2012. Interpreting variability in population biomonitoring data: role of  
579 elimination kinetics. *J Expo Sci Environ Epidemiol*. 22, 398-408.
- 580 Barraji, L., et al., 2009. Within-day drinking water consumption patterns: results from a drinking  
581 water consumption survey. *J Expo Sci Environ Epidemiol*. 19, 382-95.
- 582 Bartels, M., et al., 2012. Development of PK- and PBPK-based modeling tools for derivation of  
583 biomonitoring guidance values. *Comput Methods Programs Biomed*. 108, 773-88.
- 584 Bois, F. Y., 2000. Statistical analysis of Clewell et al. PBPK model of trichloroethylene kinetics.  
585 *Environmental Health Perspectives*. 108, 307-316.
- 586 CDC, 2009a. Centers for Disease Control and Prevention, (2009, July 13), National Environmental  
587 Public Health Tracking, Environmental Public Health Tracking & Biomonitoring.  
588 Retrieved from <http://www.cdc.gov/nceh/tracking/trackbiomon.htm>.
- 589 CDC, 2009b. Centers for Disease Control and Prevention. (2009, July 1), National Health and  
590 Nutrition Survey, 2003-2004 Laboratory Data, Polyaromatic Hydrocarbons. Retrieved  
591 from [http://wwwn.cdc.gov/nchs/nhanes/2003-2004/L31PAH\\_C.htm](http://wwwn.cdc.gov/nchs/nhanes/2003-2004/L31PAH_C.htm).

592 CDC, 2011. Centers for Disease Control and Prevention, National Health and Nutrition Survey,  
593 2009-2010 Laboratory Data, Urine Flow Rate. Retrieved  
594 from [http://www.cdc.gov/nchs/nhanes/nhanes2009-2010/UCFLOW\\_F.htm](http://www.cdc.gov/nchs/nhanes/nhanes2009-2010/UCFLOW_F.htm).

595 Clewell, H. J., et al., 2008. Quantitative interpretation of human biomonitoring data. *Toxicol Appl*  
596 *Pharmacol.* 231, 122-33.

597 Crop-Life-America, 2002. Cumulative and Aggregate Risk Evaluation System, Technical Manual.  
598 Retrieved  
599 from [http://www.epa.gov/scipoly/sap/meetings/2002/april/cares/cares\\_documentation/tmanu](http://www.epa.gov/scipoly/sap/meetings/2002/april/cares/cares_documentation/tmanual2.pdf)  
600 [al2.pdf](http://www.epa.gov/scipoly/sap/meetings/2002/april/cares/cares_documentation/tmanual2.pdf).

601 Ellison, C. A., et al., 2012. Use of Cytochrome P450-Specific Parameters and Human Biomarker  
602 Data To Develop a Human Physiologically Based Pharmacokinetic/Pharmacodynamic  
603 Model for Dermal Chlorpyrifos Exposure. *Parameters for Pesticide QSAR and PBPK/PD*  
604 *Models for Human Risk Assessment.* vol. 1099. American Chemical Society, pp. 309-322.

605 Feldmann, R. J., Maibach, H. I., 1974. Percutaneous penetration of some pesticides and herbicides  
606 in man. *Toxicol Appl Pharmacol.* 28, 126-32.

607 Georgopoulos, P. G., et al., 2009. Reconstructing population exposures to environmental chemicals  
608 from biomarkers: challenges and opportunities. *J Expo Sci Environ Epidemiol.* 19, 149-71.

609 Georgopoulos, P. G. R., A.; Gallo, M. A. , 1994. Reconstruction of short-term multi-route exposure  
610 to volatile organic compounds using physiologically based pharmacokinetic models. Journal  
611 of Exposure Analysis and Environmental Epidemiology. 4, 309-328.

612 Grulke, C. M., et al., 2013. PROCEED: Probabilistic reverse dosimetry approaches for estimating  
613 exposure distributions. Bioinformation. 9, 707-9.

614 Hinderliter, P. M., et al., 2011. Development of a source-to-outcome model for dietary exposures to  
615 insecticide residues: an example using chlorpyrifos. Regul Toxicol Pharmacol. 61, 82-92.

616 Howard, P. H., 1991. Handbook of Environmental Fate and Exposure Data for Organic Chemicals.  
617 CRC Press, Boca Raton, FL.

618 ILSI, Cumulative and Aggregate Risk Evaluation System (CARES) Version 3.0. 2009.

619 Knaak James, B., et al. (Eds.), 2012. Parameters for Pesticide QSAR and PBPK/PD Models for  
620 Human Risk Assessment. American Chemical Society.

621 Knaak, J. B., 1968. The metabolism of carbaryl in man, monkey, pig, and sheep. Journal of  
622 Agricultural and Food Chemistry. 16, 465-470.

623 Lakind, J. S., Naiman, D. Q., 2008. Bisphenol A (BPA) daily intakes in the United States: Estimates  
624 from the 2003-2004 NHANES urinary BPA data. J Expos Sci Environ Epidemiol. 18, 608-  
625 615.

626 LaKind, J. S., et al., 2014. A proposal for assessing study quality: Biomonitoring, Environmental  
627 Epidemiology, and Short-lived Chemicals (BEES-C) instrument. *Environ Int.* 73, 195-207.

628 Liao, K. H., et al., 2007. Development of a Screening Approach to Interpret Human Biomonitoring  
629 Data on Volatile Organic Compounds: Reverse Dosimetry on Biomonitoring Data for  
630 Trichloroethylene. *Risk Analysis.* 27, 1223-1236.

631 Lorber, M., 2009. Use of a simple pharmacokinetic model to characterize exposure to perchlorate. *J*  
632 *Expo Sci Environ Epidemiol.* 19, 260-73.

633 Lorber, M., et al., 2011. A critical evaluation of the creatinine correction approach: can it  
634 underestimate intakes of phthalates? A case study with di-2-ethylhexyl phthalate. *J Expo Sci*  
635 *Environ Epidemiol.* 21, 576-86.

636 Lu, C., Andres, L., 2012. Reconstructing Organophosphorus Pesticide Doses Using the Reversed  
637 Dosimetry Approach in a Simple Physiologically-Based Pharmacokinetic Model. *Journal of*  
638 *Toxicology.* 2012, 8.

639 May, D. G., et al., 1992. Cimetidine-carbaryl interaction in humans: evidence for an active  
640 metabolite of carbaryl. *J Pharmacol Exp Ther.* 262, 1057-61.

641 McNally, K., et al., 2012. Reconstruction of Exposure to m-Xylene from Human Biomonitoring  
642 Data Using PBPK Modelling, Bayesian Inference, and Markov Chain Monte Carlo  
643 Simulation. *Journal of Toxicology.* 2012, 18.

644 Meeker, J. D., et al., 2007. Utility of urinary 1-naphthol and 2-naphthol levels to assess  
645 environmental carbaryl and naphthalene exposure in an epidemiology study. *J Expo Sci*  
646 *Environ Epidemiol.* 17, 314-20.

647 Mosquin, P. L., et al., 2009. Reconstructing exposures from small samples using physiologically  
648 based pharmacokinetic models and multiple biomarkers. *J Expo Sci Environ Epidemiol.* 19,  
649 284-97.

650 Nong, A., et al., 2008. Bayesian calibration of a physiologically based  
651 pharmacokinetic/pharmacodynamic model of carbaryl cholinesterase inhibition. *J Toxicol*  
652 *Environ Health A.* 71, 1363-81.

653 NRC, 2006. National Research Council, Human Biomonitoring for Environmental Chemicals.  
654 National Research Council Committee on Human Biomonitoring for Environmental  
655 Toxicants. Washington, DC: National Academies Press.

656 NRC, 2012. National Research Council , Exposure Science in the 21st Century: A Vision and a  
657 Strategy. Washington, DC: The National Academies Press.

658 Payne-Sturges, D., et al., 2009. Evaluating Cumulative Organophosphorus Pesticide Body Burden  
659 of Children: A National Case Study. *Environmental Science & Technology.* 43, 7924-7930.

660 Phillips, M. B., et al., 2014a. A new method for generating distributions of biomonitoring  
661 equivalents to support exposure assessment and prioritization. *Regul Toxicol Pharmacol.* 69,  
662 434-42.

663 Phillips, M. B., et al., 2014b. Analysis of biomarker utility using a PBPK/PD model for carbaryl.  
664 *Front Pharmacol.* 5, 246.

665 Pleil, J. D., Sobus, J. R., 2013. Estimating lifetime risk from spot biomarker data and intraclass  
666 correlation coefficients (ICC). *J Toxicol Environ Health A.* 76, 747-66.

667 Price, P. S., et al., 2011. Application of a source-to-outcome model for the assessment of health  
668 impacts from dietary exposures to insecticide residues. *Regul Toxicol Pharmacol.* 61, 23-31.

669 Rao, B., et al., 2012. Perchlorate production by photodecomposition of aqueous chlorine solutions.  
670 *Environ Sci Technol.* 46, 11635-43.

671 Roy, A., Georgopoulos, P. G., 1998. Reconstructing week-long exposures to volatile organic  
672 compounds using physiologically based pharmacokinetic models. *J Expo Anal Environ*  
673 *Epidemiol.* 8, 407-22.

674 Sohn, M. D., et al., 2004. Reconstructing population exposures from dose biomarkers: inhalation of  
675 trichloroethylene (TCE) as a case study. *J Expo Anal Environ Epidemiol.* 14, 204-213.

676 Tan, Y.-M., et al., 2006a. Reverse dosimetry: interpreting trihalomethanes biomonitoring data using  
677 physiologically based pharmacokinetic modeling. J Expos Sci Environ Epidemiol. 17, 591-  
678 603.

679 Tan, Y.-M., et al., 2006b. Use of a Physiologically Based Pharmacokinetic Model to Identify  
680 Exposures Consistent With Human Biomonitoring Data for Chloroform. Journal of  
681 Toxicology and Environmental Health, Part A. 69, 1727-1756.

682 Ulaszewska, M. M., et al., 2012. Interpreting PCB levels in breast milk using a physiologically  
683 based pharmacokinetic model to reconstruct the dynamic exposure of Italian women. J  
684 Expos Sci Environ Epidemiol. 22, 601-609.

685 USDA, 2000. U.S. Department of Agriculture. Agricultural Research Service Continuing Survey of  
686 Food Intakes by Individuals 1994-96, 1998. CD-ROM. National Technical Information  
687 Service Accession No. PB2000-  
688 500027. <http://www.ars.usda.gov/Services/docs.htm?docid=14531>.

689 USEPA, 2004. A Model Comparison: Dietary (Food and Water) Exposure in DEEM/Calendex,  
690 CARES, and LifeLine. USEPA, OPP, Report to  
691 SAP. <http://www.epa.gov/scipoly/sap/meetings/2004/april/sapminutesapril2930.pdf>.

692 USEPA, 2006a. Organophosphorus Cumulative Risk Assessment 2006 Update. USEPA, OPP, July  
693 31, 2006. [http://www.epa.gov/pesticides/cumulative/2006-op/op\\_cra\\_main.pdf](http://www.epa.gov/pesticides/cumulative/2006-op/op_cra_main.pdf).

694 USEPA, 2006b. Triazine Cumulative Risk Assessment. USEPA, OPP, June 21,  
695 2006. [http://www.epa.gov/pesticides/cumulative/common\\_mech\\_groups.htm#triazine](http://www.epa.gov/pesticides/cumulative/common_mech_groups.htm#triazine).

696 USEPA, 2007. Revised N-methyl Carbamate Cumulative Risk Assessment. USEPA, OPP,  
697 September 24, 2007. [http://www.epa.gov/pesticides/cumulative/carbamate\\_background.htm](http://www.epa.gov/pesticides/cumulative/carbamate_background.htm).

698 USEPA and USDA, 2000. U.S. Environmental Protection Agency (USEPA), Office of Pesticide  
699 Programs and U.S. Department of Agriculture (USDA), Agricultural Research Service  
700 (2000). Food Commodity Intake Database (FCID) Version 2.1. CD-ROM. National  
701 Technical Information Service, Accession No. PB2000-  
702 500101. <http://www.ars.usda.gov/Services/docs.htm?docid=14514>.

703 Yoon, M., et al., 2015. Use of in vitro data in developing a physiologically based pharmacokinetic  
704 model: Carbaryl as a case study. *Toxicology*. 332, 52-66.

705 Yoon, M., et al., 2012. Use of *in Vitro* Data in PBPK Models: An Example of  
706 *in Vitro* to *in Vivo* Extrapolation with Carbaryl. *Parameters*  
707 for Pesticide QSAR and PBPK/PD Models for Human Risk Assessment. vol. 1099.  
708 American Chemical Society, pp. 323-338.

709 **Table 1.** Descriptions of simulations presented in this article.

710

Simulation	Description	Exposure Scenarios	Model Outputs
Sensitivity Analysis	Determine the most sensitive PBPK model parameters.	One dose per day at 2:42pm. 3 doses tested corresponding to 5 <sup>th</sup> , 50 <sup>th</sup> , and 95 <sup>th</sup> percentile of	Normalized sensitivity coefficients for the PBPK model parameters.

		CARES daily doses. 3 elapsed times between daily dose and urine sampling were tested 1, 4, and 12 hours. All other parameters were set to their means.	
Computation of biomarker concentration from model output	Two different methods for calculating biomarker concentration were compared (volume, and flow rate calculations)	Random week of intermittent exposures from food and water as specified in the CARES model for 500 virtual individuals. All other parameters were set to the synthetic individual values.	Single spot urinary 1-N concentrations based on both volume and flow rate calculations (500 each).
Synthetic intakes and biomarkers (paired data)	Model-generated corresponding dose-biomarker dataset for exposure reconstruction.	One dose per day for 5 days, dose is the mean of 365 daily doses, given at the median time when the maximum dose occurred over 365 days. Flow rate calculation was used. Parameters were set to synthetic individual values.	Paired daily intakes and corresponding spot urinary 1-N concentrations (biomarker) for 500 synthetic individuals.
Simulation for the ECF method	The dose-biomarker relationship for converting biomarker concentrations to doses in the ECF method.	1 ng/kg/day for 5 days given at the median time when the max dose occurred over 365 days. All other parameters were the same as the synthetic individuals (n=500).	500 single spot urinary 1-N concentrations based on the flow rate calculation compared to synthetic biomarkers, to estimate the intake distribution.
Simulation for the DBA method	The dose-biomarker relationship for converting biomarker concentrations to doses in the DBA method.	Intake doses ranged from $10^{-2}$ to $10^6$ ng/kg/day, incrementing on a $\log_{10}$ -scale by $10^{0.08}$ ( $N=101$ ), each dose was repeated for 5 days. All other parameters were the same as the synthetic individuals (n=500).	500 single spot urinary 1-N concentrations based on the flow rate calculation (for each of the 101 intakes), which were compared to synthetic biomarkers, to estimate the intake distribution.
MCMC for Method Comparison, all parameters known.	In a single MCMC iteration: For each updated prior of exposures, biomarkers are predicted for the population and compared to the synthetic biomarkers.	One dose per day for 5 days, given at the median time when the max dose occurred over 365 days. The distribution of exposure dose is updated at each step of the MCMC. All other parameters were the same	Single spot urinary 1-N concentrations (based on the flow rate calculation, n=500 per MCMC iteration), compared to synthetic biomarkers to

		as the synthetic individuals (n=500)	estimate posterior distribution of intakes.
MCMC, for testing different parameters of interest: Case 1, All parameters set at their mean.	For each updated prior of exposures, biomarkers are predicted for the population and compared to the synthetic biomarkers.	One dose per day for 5 days, given at the median time when the max dose occurred over 365 days. The distribution of exposure dose is updated at each step of the MCMC. All parameters, including the time of sampling, were set to their respective means.	500 single spot urinary 1-N concentrations (based on the flow rate calculation), per MCMC iteration. These biomarker concentrations were compared to the synthetic biomarkers to estimate posterior intake distribution.
MCMC, for testing different parameters of interest: Case 2 (Default)	Same as above.	Same as above, except that the parameter of interest was set to known individual values, and all other parameters were set to their mean.	Same as above.
MCMC, for testing different parameters of interest: Case 3 (Random)	Same as above.	Same as above, except that the parameter of interest was set to randomly selected individual values from a distribution, and all other parameters were set to their mean.	Same as above.

711

712

713 **TABLE 2.** Comparing the geometric means and geometric standard deviations for carbaryl intake  
714 dose estimated from CARES against those reconstructed using the Exposure Conversion Factor  
715 (ECF), the Discretized Bayesian Approach (DBA) using the both the uniform prior and the biased  
716 prior, and Markov Chain Monte Carlo (MCMC) methods.

	Geo. Mean (ng/kg/day)	Geo. Std. Dev.
CARES-synthetic daily intake	70	4.1
ECF-reconstructed daily intake	97	787
DBA-reconstructed daily intake (uniform)	100	795
DBA-reconstructed daily intake (biased)	251	663
MCMC-reconstructed daily intake	92	4.5

717

718

719 **Table 3.** Comparing the geometric means and geometric standard deviations for carbaryl intake  
 720 dose estimated from CARES against those reconstructed from Markov Chain Monte Carlo  
 721 (MCMC) methods assuming either all parameters were known (from method comparison analysis)  
 722 or set to their respective means (Case 1). Six additional MCMC trials were also included for  
 723 comparison: setting elapsed time between the last dose and urine sampling (Elapsed Time), urine  
 724 flow rate, or urinary elimination rate to either the values used to generate the 1-naphthol (1-N)  
 725 concentrations in urine (Case 2, default), or to values generated from random sampling from a  
 726 distribution (Case 3, random).

727

	Geo. Mean (ng/kg/day)	Geo. Std. Dev.
CARES-synthetic daily intake	70	4.1
MCMC – all parameters known	92*	4.5
MCMC – all parameters set at their means	47	0.8
<b>Elapsed Time</b>		
MCMC – default	393*	59
MCMC – random	690*	116
<b>Urine Flow Rate</b>		
MCMC – default	352*	67
MCMC – random	45,968*	30,055
<b>Urinary Elimination Rate</b>		
MCMC – default	508*	93
MCMC – random	507*	83

728 \* indicates that the mean is significantly different than the mean of the CARES-synthetic

729 distribution, using a Welch t-test with a 0.05 significance level.

730

731 **Figure Legend**

732

733 **Figure 1.** Probability density of carbaryl intake (ng/kg/day) for 500 simulated individuals. The x-  
734 axis has been  $\log_{10}$  transformed. The black boxes show the histogram of the carbaryl intake doses  
735 generated using the CARES model that served as the input data for the PBPK simulation. The  
736 blue dashed-dotted line shows the lognormal distribution that was fitted to the carbaryl intake data.

737 **Figure 2.** Effect of the prior distribution on the results of Discretized Bayesian Analysis (DBA) for  
738 reconstructing intakes of carbaryl (ng/kg/day). (A) Uniform DBA prior (red dashed line); the  
739 corresponding estimate from DBA (solid black line); simulation input (from Figure 1, dashed-dotted  
740 blue line) shown for comparison. (B) Biased DBA prior: lognormal distribution (geometric mean:  
741  $10^3$  ng/kg/day; geometric standard deviation:  $\sqrt{10}$ ) truncated at  $10^{-2}$  (lower bound) and  $10^6$  (upper  
742 bound) (red dashed line); the corresponding estimate from DBA (solid black line); simulation input  
743 (from Figure 1, dashed-dotted blue line) shown for comparison.

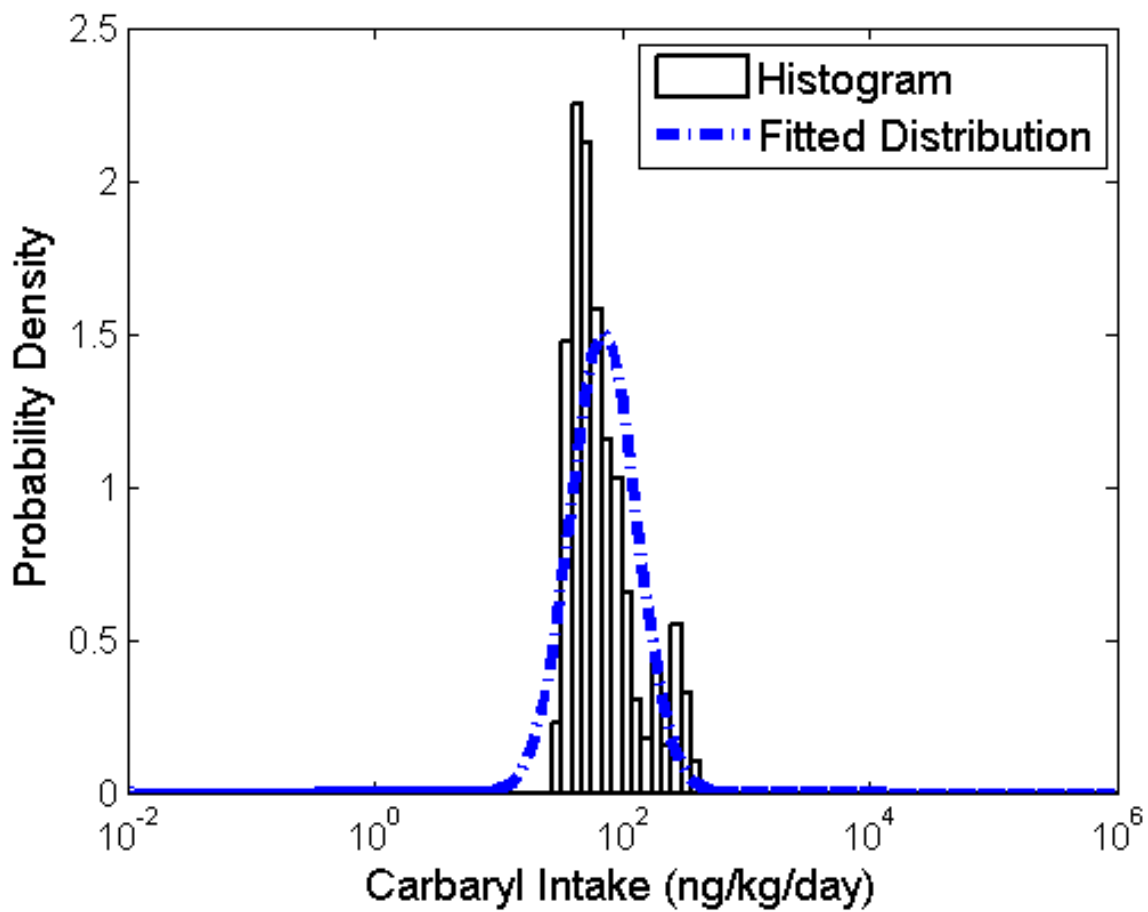
744

745

746

747 **Figure 1**

748

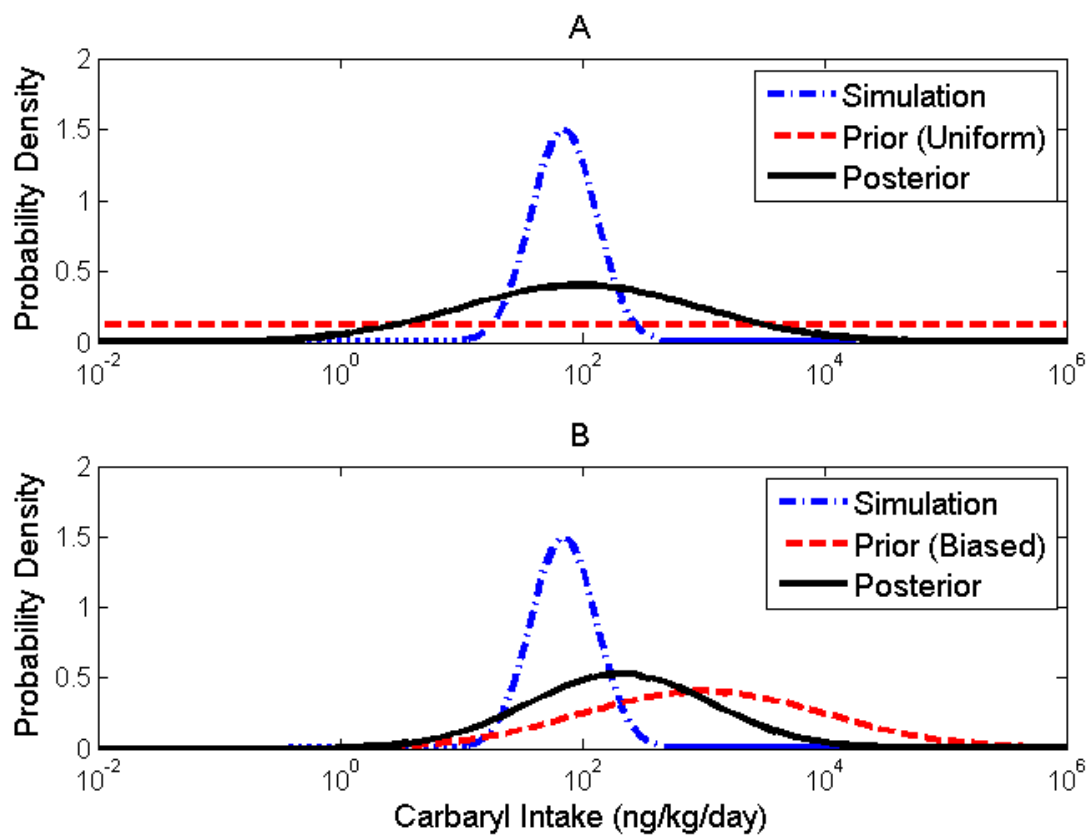


749

750

751 **Figure 2**

752



753